International Journal of Mechanical, Industrial and Aerospace Sciences
ISSN: 2517-9950
Vol:11, No:6, 2017

Hybrid Quasi-Steady Thermal Lattice Boltzmann Model for Studying the Behavior of Oil in Water Emulsions Used in Machining Tool Cooling and Lubrication

W. Hasan, H. Farhat, A. Alhilo, L. Tamimi

Abstract**—**Oil in water (O/W) emulsions are utilized extensively for cooling and lubricating cutting tools during parts machining. A robust Lattice Boltzmann (LBM) thermal-surfactants model, which provides a useful platform for exploring complex emulsions' characteristics under variety of flow conditions, is used here for the study of the fluid behavior during conventional tools cooling. The transient thermal capabilities of the model are employed for simulating the effects of the flow conditions of O/W emulsions on the cooling of cutting tools. The model results show that the temperature outcome is slightly affected by reversing the direction of upper plate (workpiece). On the other hand, an important increase in effective viscosity is seen which supports better lubrication during the work.

Keywords**—**Hybrid lattice Boltzmann method, Gunstensen model, thermal, surfactant-covered droplet, Marangoni stress.

I. Introduction

REDUCING the friction between the cutting tool edge and workpiece and controlling the temperature and corrosion are the main functions of cutting fluid. As temperature increases to high levels, tool wear will be supported which has negative effects on tool life and machining accuracy [1]. About 15–25% of production total cost is spent for coolant [2].

Yakup and Nalbant [3] investigated a cooling method, which uses liquid nitrogen in the procedure of material removal and studied its effects on cutting tool and workpiece material properties. The authors concluded that using liquid nitrogen cooling is one of the most favorable method for material cutting operations, because it can improve tools' life and surface finish by reducing tools' wear resulting from a proper control of the machining temperature.

Sharma et al. [4] proposed an overview of major advances in techniques used to minimize the amount of lubricant such as compressed air cooling, solid coolants-lubricants, cryogenic cooling, and high pressure coolant. These techniques led to increasing productivity, minimizing friction, and heat generation.

Haq and Tamizharasan [5] proposed the use of heat pipe during machining and they studied the effects of different heat pipe parameters such as length, diameter degree of vacuum, and material of heat pipe. They assumed that the cutting tool is subjected to static heating in the cutting zone, which verifies the analysis and practicality of using this cooling method in turning operations. Taguchi's Design of Experiments was used for optimizing the heat pipe parameters and a confirmation test was conducted by using the fabricated heat pipe with the best values of parameters. The results of the study showed a reduction by about 5% in temperature. This leads to an improved cutting tool life, surface finish, and minimization of wear. The finite element analysis results also projected a reduction in temperature in the cutting zone and that the heat flow to the tool is effectively removed when a heat pipe is used.

Komanduri and Hou [6] presented an analytical model, which extends Jaeger's [7], [8] approximate solution of a moving-band heat source for the chip and a stationary rectangular heat source for the tool for metal cutting. Appropriate boundary conditions and a non-uniform heat distribution along the tool were assumed. The calculated temperature showed an increasing in temperature distribution on the two sides of the tool and chip interface showed good agreements for the two cases.

Komanduri and Hou [9] proposed a model which deals with the temperature rise distribution in metal cutting due shear plane heat source in the primary shear zone and frictional heat source at the tool-chip interface. The model was used for two cases of metal cutting. The analytical results were found to be in good agreement with the experimental results, thus validating the model.

In this work, a different approach is suggested for studying tools' cooling. This approach focuses on attempting to understand the physics of the multiphase coolant, i.e. its transport properties relation with the flow conditions imposed during the cooling process to improve the process. Complex multiphase thermal-surfactants LBM, which couples the energy equation with hydrodynamics and interface physics, is used in the simulation of the cooling of cutting tool using O/W emulsions (SAE-50 oil and water).

II. Numerical Method

A. LBM and the Gunstensen Model

The Bhatnagar-Gross-Krook (BGK) LBM isothermal,

W. Hasan is with the North Oil Company, Kirkuk, Iraq and Department of Mechanical Engineering, Wayne State University, Detroit, MI, USA (e-mail: fk1029@wayne.edu).

H. Farhat, A. Alhilo and L. Tamimi are with the Department of Mechanical Engineering, Wayne State University, Detroit, MI, USA.

single-relaxation model used in this work is derived from the Boltzmann kinetic equation:

$$\frac{df}{dt}+\boldsymbol{\xi}\cdot\nabla f=-\frac{1}{\lambda}(f-f^{eq}) \tag{1}$$

where f is the density distribution function, $\boldsymbol{\xi}$ is the macroscopic velocity, f^{eq} is the equilibrium distribution function, and λ is the physical relaxation time. Equation (1) is first discretized by using a set of velocities $\{\xi_i\}$ confined to a finite number of directions and this leads to:

$$\frac{df_i}{dt}+\boldsymbol{\xi}_i\cdot\nabla f_i=-\frac{1}{\lambda}(f_i-f_i^{eq}) \tag{2}$$

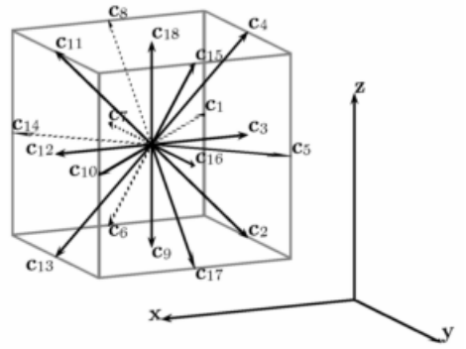

Fig. 1 Velocity vectors for the D3Q19 lattice Boltzmann method used in this model

In the multi-component LBM, (2) is further discretized in the lattice space and time and this leads to the following:

$$\tilde{f}_i^{\,q}(x,t+\delta_t)=f_i^{\,q}(x,t)-\frac{1}{\tau^q}[f_i^{\,q}(x,t)-f_i^{\,q,eq}(\rho,\rho u)]+\phi_i(x) \tag{3}$$

The lattice space δ_x and the lattice time step δ_t are taken as unity and their ratio $c=\delta_x/\delta_t=1$, while q refers to the light and heavy fluids.

$$\nu=(\tau-0.5)c_s^2\delta_t \tag{4}$$

The Gunstensen multi-component model uses a color blind total density distribution function given by:

$$f_i(\boldsymbol{x},t)=f_i^{\,L}(\boldsymbol{x},t)+f_i^{\,H}(\boldsymbol{x},t) \tag{5}$$

$$\rho^N(\boldsymbol{x},t)=\frac{\rho^L(\boldsymbol{x},t)-\rho^H(\boldsymbol{x},t)}{\rho^L(\boldsymbol{x},t)+\rho^H(\boldsymbol{x},t)}$$
$$\rho^L(\boldsymbol{x},t)=\sum_0^{Q-1}f_i^{\,L}(\boldsymbol{x},t);\rho^H(\boldsymbol{x},t)=\sum_0^{Q-1}f_i^{\,H}(\boldsymbol{x},t) \tag{6}$$

The streaming step comes after the segregation of the fluids by:

$$f_i^{\,L}(\boldsymbol{x}+\boldsymbol{c}_i\delta_t,t+\delta_t)=\tilde{\tilde{f}}_i^{\,L}(\boldsymbol{x},t+\delta_t)$$
$$f_i^{\,H}(\boldsymbol{x}+\boldsymbol{c}_i\delta_t,t+\delta_t)=\tilde{\tilde{f}}_i^{\,H}(\boldsymbol{x},t+\delta_t) \tag{7}$$

The macroscopic density and momentum are obtained from the distribution function as:

$$\rho=\sum_{i=0}^{Q-1}f_i=\sum_{i=0}^{Q-1}f_i^{eq} \tag{8}$$

$$\rho\boldsymbol{u}=\sum_{i=1}^{Q-1}\boldsymbol{c}_i f_i=\sum_{i=1}^{Q-1}\boldsymbol{c}_i f_i^{eq} \tag{9}$$

B. The Surfactant Model

The general time-dependent surfactant convection-diffusion equation is given by:

$$\partial_t\Gamma+\nabla_s\cdot(\boldsymbol{u}_s\Gamma)+K\Gamma u_n=D_s\nabla_s^2\Gamma \tag{10}$$

where $\partial_t\Gamma$ accounts for the temporal change in the interface surfactant concentration, $\nabla_s\cdot(\boldsymbol{u}_s\Gamma)$ is the convection term, $k\Gamma u_n$ is to describe the effects of change in the interface morphology on the surfactant concentration distribution, and $D_s\nabla_s^2\Gamma$ is the diffusion term.

C. The Quasi-Steady Thermal Model

Assuming small variations in the thermal fluid properties and no phase change due to temperature rise or fall, the following energy equation is used for the calculation of the flow temperature profile:

$$\partial_t T+\nabla\cdot(\boldsymbol{u}T)=D_{ifs}\nabla^2T+\varphi \tag{11}$$

In (11), $\partial_t T$ accounts for the fluid temperature change in time, $\nabla\cdot(\boldsymbol{u}T)$ is the convection term, and $D_{ifs}\nabla^2T$ is the diffusion term, φ accounts for the flow viscous dissipation.

D. The Hybrid Thermal-Surfactants Model

The proposed Gunstensen LBM is used for determining the hydrodynamic characteristics of the mixture and for tracking the fluid-fluid interface. During initialization of the LBM, the initial surfactant concentration Γ_i is imposed on the interface with a controllable thickness. The thermal boundary condition is also applied during this step.

After determining the LBM velocity components (u_x,u_y,u_z), the droplet curvature and the interface normal

components $\left(k, n_x, n_y, n_z\right)$, the tangential components $\left(u_{sx}, u_{sy}, u_{sz}\right)$ of the interface velocity are calculated. These variables are thereafter used for the derivation of the surfactant-diffusion, and the governing energy equation. Both equations are solved by a finite difference scheme resolved on the same spatial lattice grid.

The coupling back of the thermal and surfactant effects on the fluid LBM is executed in the following order:

The temperature dependent surface tensions of both fluids are updated by:

$$\alpha_q^{(T)} = \alpha_{q,0}\left(1+\frac{T_0}{T_{c,q}-T_0}\right)\left(1-\frac{T}{T_{c,q}}\right)^n \tag{12}$$

The temperature dependent interfacial tension is then calculated by:

$$\alpha_0^{(T)} = \alpha_a^{(T)} + \alpha_b^{(T)} - 2\phi\sqrt{\alpha_a^{(T)}\alpha_b^{(T)}} \tag{13}$$

The temperature dependent surfactant elasticity is determined by:

$$E_o^{(T)} = \frac{E_0 T}{T_0} \tag{14}$$

The final update of the interfacial tension is given by:

$$\alpha = \alpha_0^{(T)}\left[1+E_0^{(T)}\ln\left(1-\Gamma^*\right)\right] \tag{15}$$

III. Simulation and Discussion

A domain consisting of $145\times65\times125\left[lu^3\right]$ is used in the succeeding simulations. Geometrical similarity of 125 lattice units for 2.5×10^{-4} meters is utilized.

The surfactant covered droplets initial radii are set to $R_0 = 15\left[lu\right]$. Shear rate of $1.27\times10^{-7} \le \dot{\gamma} \le 1.27\times10^{-5}\left[ts^{-1}\right]$ is imposed through moving the top wall with respect to the stationary bottom wall in the direction shown in Fig. 1 by the following equation:

$$\boldsymbol{u}^{\infty}\left(\boldsymbol{x}\right) = \begin{pmatrix} 0 & 0 & -\dot{\gamma} \\ 0 & 0 & 0 \\ 0 & 0 & 0 \end{pmatrix}\cdot\boldsymbol{x} \tag{16}$$

A. Transient Thermal Case Study

Emulsions of O/W are used extensively during parts machining for simultaneous cooling and lubrication of the parts and the cutting tools. In this simulation, a mixture with volume fraction $\phi_{o/w} \approx 10\%$ is used for simulating the conditions of cooling and lubrication during machining. Simple shear flow with pressure gradient (Couette flow) can be observed in a simple hypothetical case of linear milling of a piece of metal, where cooling is generously provided both externally and internally between the cutting tool and the part to avoid extreme temperatures of the cutting tool and to prevent coolant phase change. This simple case can be simulated by Couette flow. This simulation is to investigate the effects of the driving flow pressure gradients and flow direction with respect to the cutting tool direction of movement, on the resulting coolant outlet temperature and its relative viscosity. In case of an undisturbed flow between two parallel plates the pressure gradient per unit length leads to the following average velocity:

$$V_{av} = \frac{h^2\Delta p}{3W\mu\ell} \tag{17}$$

The viscosity used in (4) is that of the suspending fluid at an initial fluid average temperature of 25 °C resulting and wall temperature of 80 °C. This equation helps calculating a reference average velocity for comparison with the velocity of the top wall for dimensionless analysis of the posed problem. The resulting dimensionless velocity is given by $U_{ds} = V_{av}/U$, which indicates the ratio of the undisturbed velocity between two parallel plate and the velocity of the top wall in a simple shear flow.

Two values for pressure drop per unit length are used with the top plate moving in opposite directions, which leads to the following four conditions characterized by $U_{ds} = \pm0.142$ and $U_{ds} = \pm0.284$. The dimensionless time is calculated by multiplying the lattice time step with the shear strain rate due to the top plate movement as $T_{ds} = T_{lat}\dot{\gamma}$.

From Fig. 2, it is clear that reversing the top plate direction has a little effect on the temperature outcome; however, in both pressure gradient cases, the relative viscosity is substantially higher when the pressure driven flow is counter acting the effect of the top plate movement (counter flow). A careful observation of (14) used in the calculation of the effective viscosity is helpful in explaining this rheological behavior. In the case of counter flow condition, the volumetric flow rate is much smaller than that of the opposite condition. Since the effective viscosity is inversely proportional to the volumetric flow rate, it is expected that the viscosity will increase upon a decrease in flow rate. It is important to state that under counter flow condition the pressure drop is higher than that of the parallel flow. This should contribute to an increase in the effective viscosity since it is directly proportional to the pressure drop; however, the magnitude of increase in the pressure drop is not comparable to that of decrease in the flow rate.

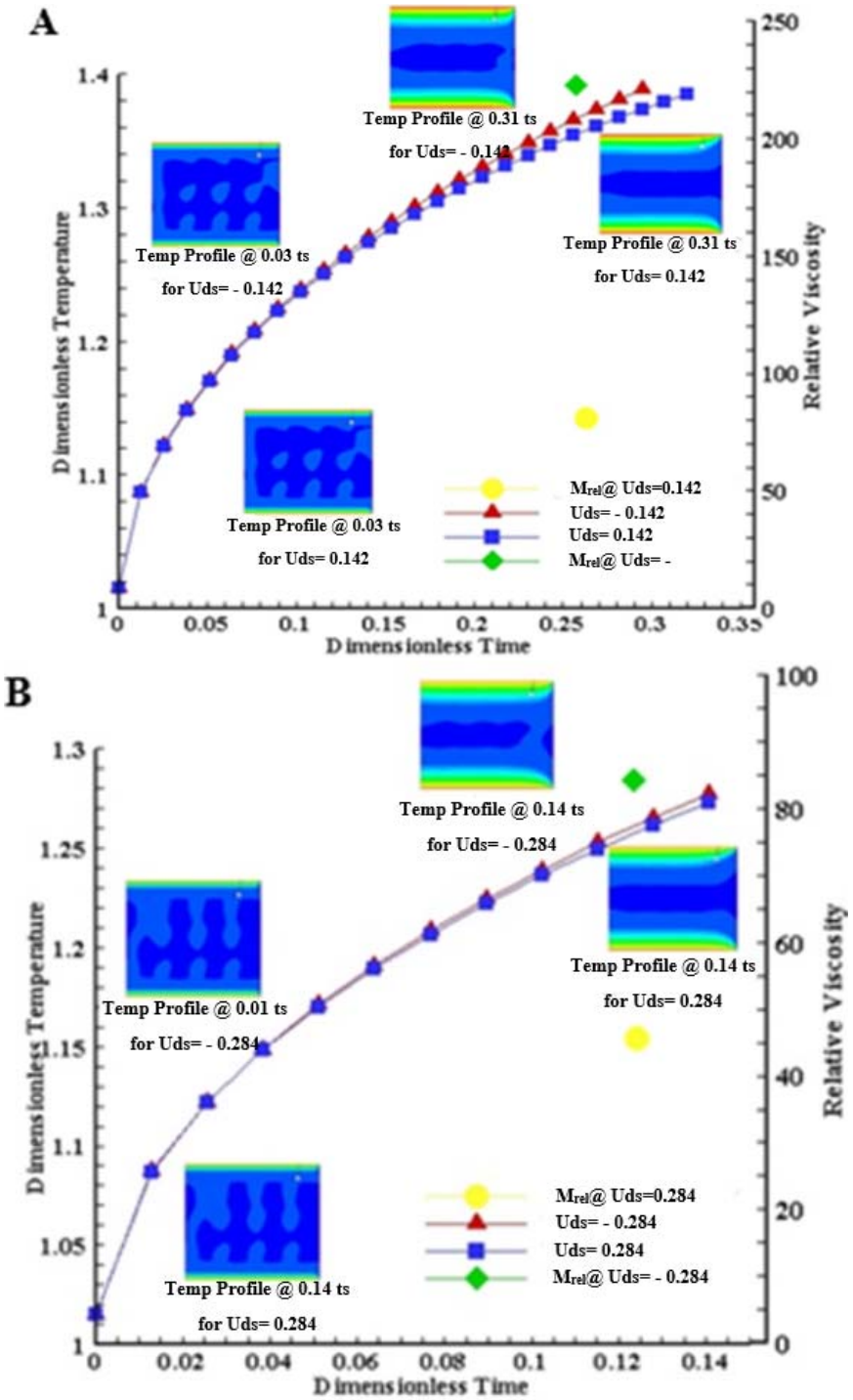

Fig. 2 Temperature profile as a function of dimensionless time as prescribed in the text and evaluation of the relative viscosities for all cases at determined dimensionless time. The insets are for the temperature contours. A- for upper plate velocities=∓0.142, B- for upper plate velocities=∓0.284

Comparing the temperature profiles and relative viscosities in Fig. 2 leads to the conclusion that the outlet temperatures for the higher dimensionless velocity U_{ds} cases are slightly lower and that has to do with the emulsion smaller residence time inside the channel. The relative viscosity is higher for lower dimensionless U_{ds} cases due to lower volumetric flow rate.

The heat rejection in all cases can be assessed by:

$$\dot{Q} = \rho Q c_p \Delta T \tag{18}$$

The results from the simulations show that it is practical to use counter flow configuration to ensure better lubricity during machining. It is also beneficiary to increase the flow rate since the heat rejection ratio for the two counter flow cases is calculated at dimensionless $T_{ds} = 0.1408$ as follows:

$$R_{\dot{Q}} = \frac{\dot{Q}_{U_{ds}=-0.284}}{\dot{Q}_{U_{ds}=-0.142}} = 3.07 \tag{19}$$

The surfactant distribution on the droplets is shown in Fig. 3. The simulation conditions show dominance of the top wall velocity compared to the flow velocity due to pressure gradient per unit length.

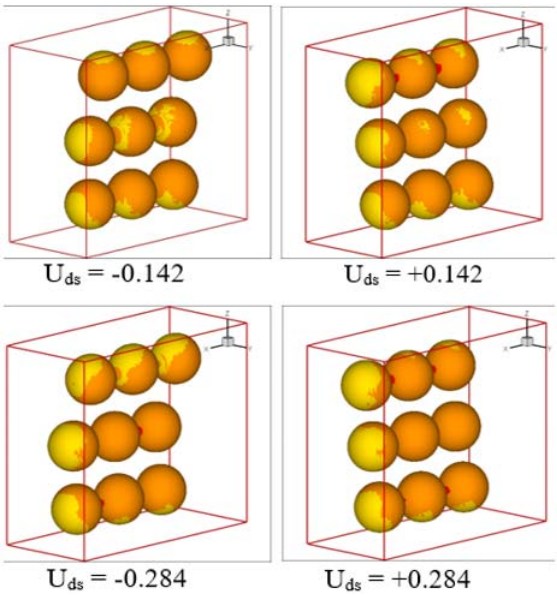

Fig. 3 Surfactant distribution at same dimensionless time $T_{ds} = 0.1408$ for the four different dimensionless velocities

B. Surfactant Distribution for Transient Thermal Case Study

It is shown from Fig. 3, that the distribution of surfactant on the droplets in the simulation domain are mainly affected by the presence of the moving and the stationary walls. The following observations can be reported:

a- The upper surfaces of the top three droplets are subjected to higher shear flow with negative top wall velocity. This is evident from the diminishing surfactants concentration at the top surface. The effect is less influential with the top plate moving in the positive direction. In the case of higher flow driving pressure gradient, the reduction of surfactant concentration start affecting the rear surface due to the fact that the droplets tend to resist the movement in the direction of the top plate.

b- The bottom surfaces of the bottom three droplets are mainly affected by the pressure gradient induced flow and they are indifferent to the top wall motion and its direction. The surfactants concentration distribution is almost identical in all cases. The last bottom droplets show concentration decrease at the rear surface, which is due to the flow expanding towards the periodic boundary.

c- The two central frontal droplets at low pressure gradient driven flow show some surfactant concentration reduction at the rear and top side surfaces depending on the movement direction of the top plate. This is an indication of the influence of the top wall movement on the surfactants distribution. This is not observed with the higher pressure gradient because in the case of negative top wall velocity, the pressure induced pressure neutralizes the effects of the top wall. In the case of positive top wall velocity, the absence of walls does not allow a change in the surfactants concentration. The rear central droplets show consistent decrease in surfactants concentration due to the pressure induced flow expansion at the periodic boundary.

IV. Conclusion

A quasi-steady thermal-surfactants hybrid Boltzmann model is used for studying the effects of O/W emulsion flow conditions on the cooling of cutting tool. The results of the transient simulation are reasonable and that show that:

a- Reversing the top plate direction has a little effect on the temperature outcome.

b- The relative viscosity and pressure drop is clearly higher for the counter flow case which supports better lubrication during the process.

c- Surfactant distribution on the droplets in the simulation domain is affected by the presence of the moving and the stationary walls.

Acknowledgment

The authors would like to thank The Higher Committee for Education Development in Iraq (HCED) for their financial support.

References

[1] Vincent Dessoly, Shreyes N. Melkote, Christophe Lescalier (2004) Modeling and verification of cutting tool temperatures in rotary tool turning of hardened steel. International Journal of Machine Tools and Manufacture 44:1463–1470.

[2] Jen TC, Gutierrez G, Eapen S, Barber G, Zhao H, Szuba PS, Lambataille J, Manjunathaiah J (2002) Investigation of heat pipe cooling in drilling application, part 1. Preliminary numerical analysis and verification. International Journal of Machine Tools and Manufacture 43:643–652.

[3] Yakup Yildiz, Muammer Nalbant (2008) A review of cryogenic cooling in machining processes. International Journal of Machine Tools and Manufacture 48:947–964.

[4] Vishal S. Sharma, Manu Dogra, N.M. Suri c (2009) Cooling techniques for improved productivity in turning. International Journal of Machine Tools and Manufacture 49:435–453.

[5] A.Noorul Haq, T. Tamizharasan (2006) Investigation of the effects of cooling in hard turning operations. International Journal of Manufacturing Technology 30: 808–816.

[6] Ranga Komanduri, Zhen Bing Hou (2001) Thermal modeling of the metal cutting process Part II: temperature rise distribution due to frictional heat source at the tool chip interface. International Journal of Mechanical Sciences 43:57-88.

[7] Jaeger JC (1942) Moving sources of heat and the temperature at sliding

contacts. Proceedings of the Royal Society of New South Wales 76,202.
[8] Carlsaw HS, Jaeger JC (1959) Conduction of heat in solids. Oxford, UK: Oxford University Press.
[9] Ranga Komanduri, Zhen Bing Hou (2001) Thermal modeling of the metal cutting process Part III: temperature rise distribution due to the combined effects of shear plane heat source and the tool-chip interface frictional heat source. International Journal of Mechanical Sciences 43: 89-107.